Supplementary data for ***JBC/2020/015956***

Critical roles of mitochondrial tyrosyl-tRNA synthetase in oxidative phosphorylation systems and vision function

Xiaofen Jin[1,2,3†], Zengming Zhang[3†], Zhipeng Nie[3], Chenghui Wang[3], Feilong Meng[2,3], Qiuzi Yi[3], Mengquan Chen[4], Jiji Sun[3], Jian Zou[5], Pingping Jiang[2,3,6]*, and Min-Xin Guan[1,2,3,6,7]*

Supplementary Methods for immunofluorescence staining

Supplemental Figure S1, S2, S3, S4, S5 and S6

Supplementary Methods

Immunofluorescence analysis for subcellular co-localization (Fig.S3)

Hela cells were cultured on cover glass slips (Thermo Fisher), and transiently transfected by plasmids carrying YARS2-Flag, NDUFA9-Flag and YARS2-HA using Hieff Trans™ Liposomal Transfection Reagent, respectively. After culturing for 20hours, cells were then fixed in 4% formaldehyde for 15 min, permeabilized with 0.2%Triton X-100, blocked with 5% goat serum for 1 h at room temperature, and immunostained with Flag (GNI) and CO2 (Proteintech), Flag and NDUFS1 (Proteintech), Flag and HA (Abcam), Flag and NDUFS3 (Proteintech) antibodies diluted in PBS with 5% goat serum overnight at 4°C, respectively. The cells were then incubated with Alex Fluor 594 goat anti-mouse IgG (H+L) (Thermo Fisher) and Alex Fluor 488 goat anti-rabbit IgG (H+L) (Thermo Fisher) for 1 h at room temperature, and nuclear were stained by DAPI, and then mounted with Fluoromount (Sigma-Aldrich). Cells were examined using a confocal fluorescence microscope (Olympus Fluoview FV1000, Japan) with three lasers (Ex/Em = 405/461, 473/520, 559/618). The acquired images were processed in Fiji, the Co-localization, Coloc 2 plug-in was used to assess the co-localization efficiency of YARS2 with CO2, NDUFS1, NDUFA9, and NDUFS3, respectively.

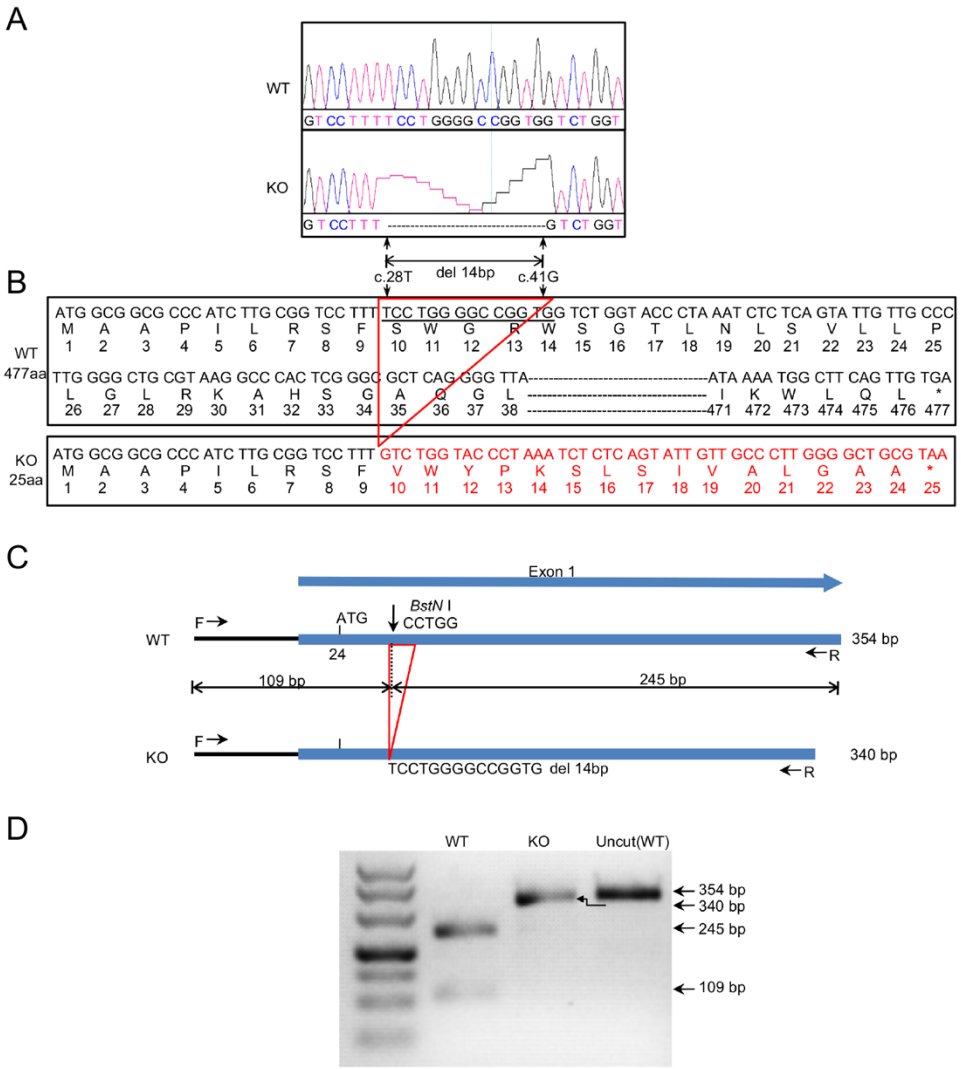

Figure S1 (related to Fig. 2). Confirmation of *YARS2*-knockout (*YARS2*^{del14bp}) allele. (A) Partial sequence chromatograms of exon I in the *YARS2* gene in the HeLa cell line (WT) and resultant *YARS2*^{KO} cell line (KO). The arrow indicates the location of the nucleotide changes at position 23. (B) Partial nucleotide sequence and amino acid sequence of *YARS2* gene in WT and MT. (C) Schema for designing restriction fragment length polymorphism (RFLP) with digested with *Bst*NI. PCR amplified for 354 bp fragment spanning partial promoter region and exon 1 were digested by *BstNI*. In fact, the *YARS2*^{14bpdel} mutation abolished the site of *BstNI*. After *BstNI* digestion, 354 bp PCR segments of WT resulted in 109 bp and 245 bp fragments, respectively. The forward and reverse primers for this genotyping analysis were 5'-ACCTTCCCTAGGAGCTGTAAGTAG-3' and 5' AGATGACCCACATGAAGCGAGTC- 3', respectively.
(D) RFLP analysis for WT and MT. Genotyping for the *YARS2*^{del14bp} mutation was carried out by PCR amplification of DNA segments in WT and MT cell lines and by digestion of the 354 bp segment with the restriction enzyme *BstNI*. Uncut (WT) indicated the PCR segment from WT. The resultant products were separated by 1% agarose gel electrophoresis.

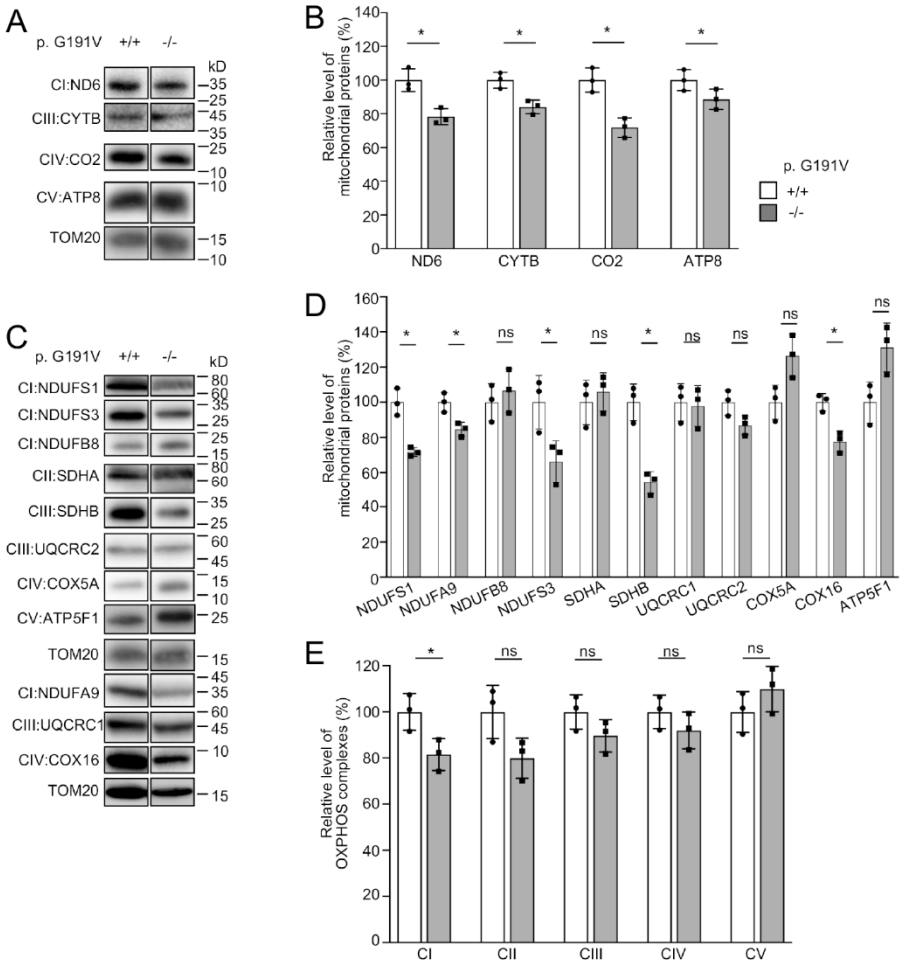

Figure S2 (related to Fig. 2). Western blotting analysis of mitochondrial proteins in lymphoblast cell line carrying the homozygous YARS2 p.G191V mutation (I-1) and control line (A61) lacking the mutation. (A, C) Twenty micrograms of total cellular proteins from various cell lines were electrophoresed through a denaturing polyacrylamide gel, electroblotted and hybridized with antibodies for 15 subunits of OXPHOS (4 encoded by mtDNA and 10 encoded by nuclear genes), and TOM20 as a loading control. (B,D,E) Quantification of mitochondrial proteins. The levels of proteins in mutant and control cell lines were determined as described elsewhere[31]. Average levels of 4 mtDNA encoding subunits (B), 10 nucleus-encoding subunits (D)， and (E) Average levels of subunits of each complex of OXPHOS (4 of complexes I, 1 of II, 3 of III, 3 of IV and 3 of V) measured above. The calculations were based on three independent determinations. The error bars indicate two standard deviations (SD) of the means. *, P<0.05; **, P<0.001; ***, P<0.0001; ns, no significant.

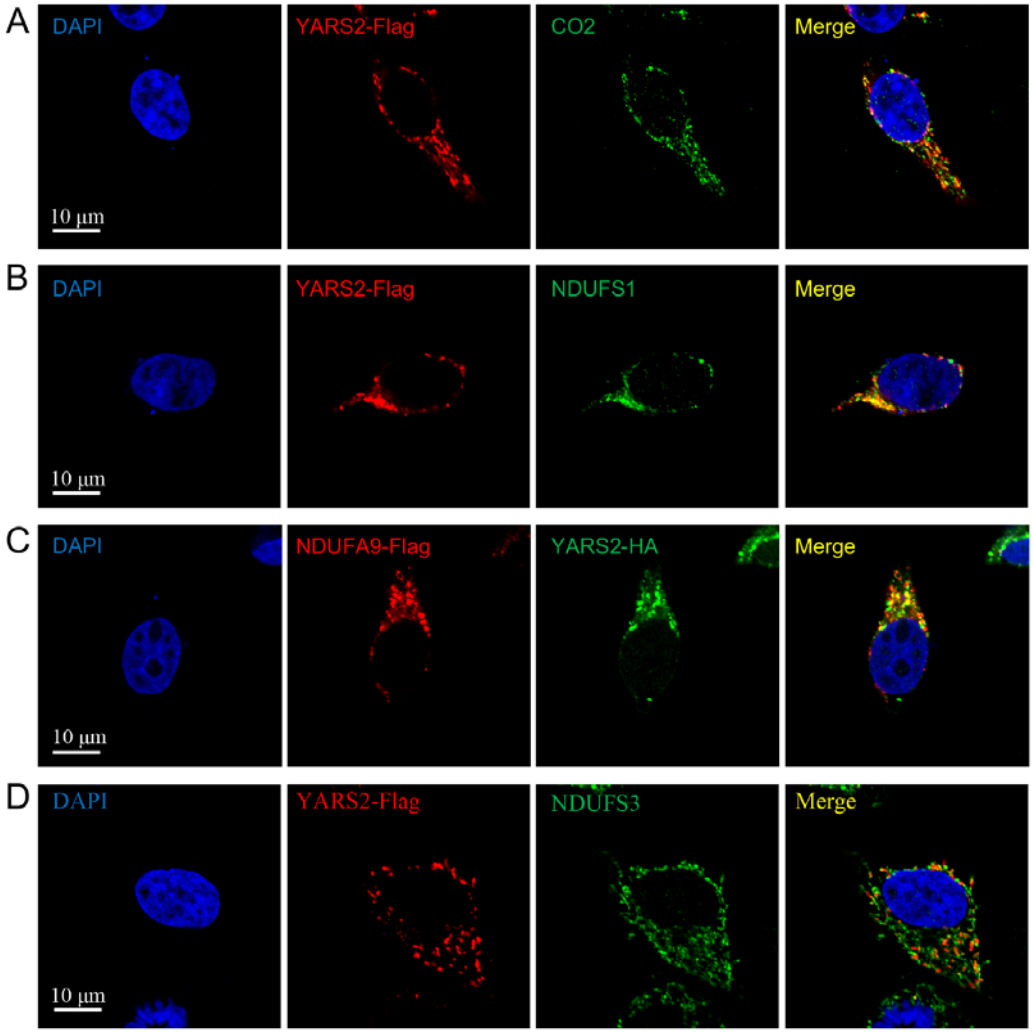

Figure S3 (related to Fig 5). Co-localization of YARS2 by Immunofluorescence staining. (A) Co-localization of YARS2-Flag (red) and CO2 (green). Pearson's correlation coefficient r=0.59. Scale bars, 10 μm. (B) Colocalization of YARS2-Flag (red) and NDUFS1 (green). Pearson's correlation coefficient r=0.71. Scale bars, 10 μm. (C) Co-localization of NDUFA9-Flag (red) and YARS2-HA (green). Pearson's correlation coefficient r=0.73. Scale bars, 10 μm. (D) Colocalization of YARS2-Flag (red) and NDUFS3 (green). Pearson's correlation coefficient r=0.405. Scale bars, 10 μm.

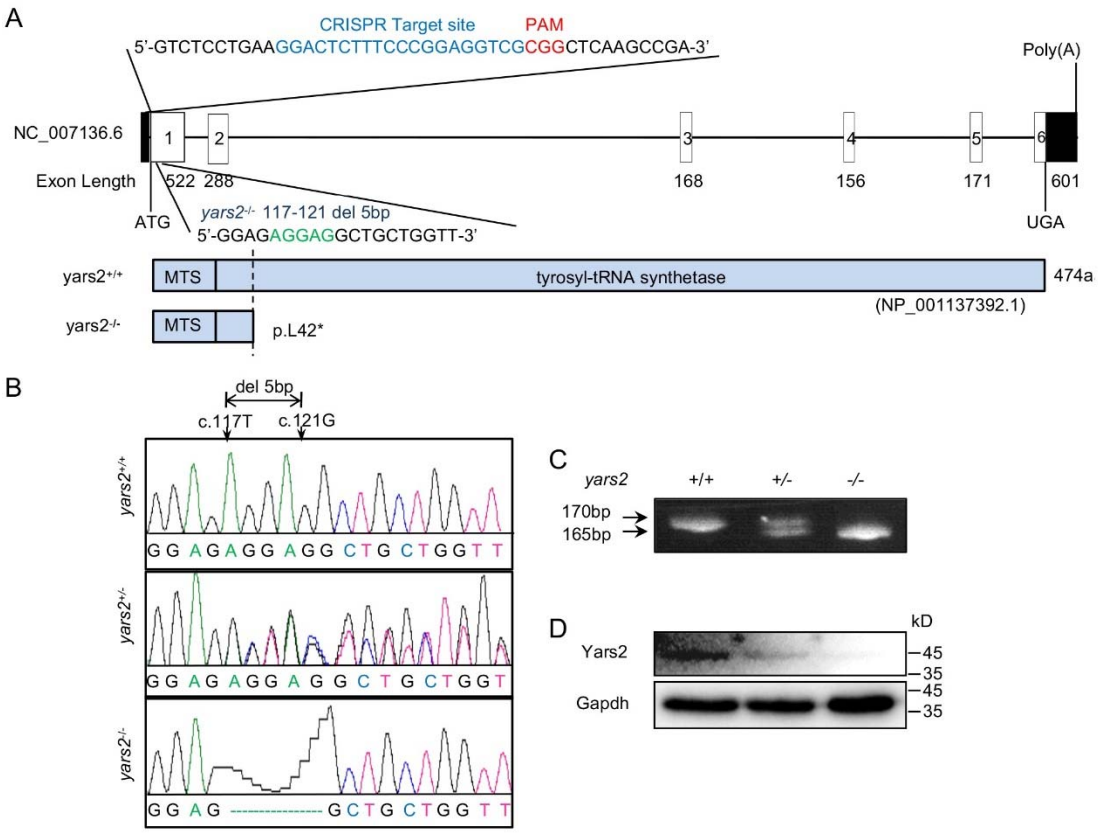

Figure S4 (related to Fig. 7). Generation of *yars2* knockout zebrafish. (A) Schematic representation of CRISPR/Cas9 target site at the exon 1 of zebrafish *yars2* gene as used in this study. A 5 bp deletion in the exon 1 was generated, resulting in a stop codon at codon 42 (p.L42*) and truncated 41 amino acid protein (p.L42*). (B) Partial sequence chromatograms of exon 1 in the *yars2* gene in the *yars2*$^{+/-}$, *yars2*$^{-/-}$, and wild type as *yars2*$^{+/+}$ Zebrafish. The arrow indicates the location of the nucleotide changes at position 23. (C) PAGE analysis of PCR products. The genotyping for the *yars2*^{5bpdel} mutation in each fishes was PCR amplified for the DNA segments in the partial exon 1 (170 bp for WT) and (165bpfor MT) with two primers: 5'-:AAACATCCGCCAAACCTCCC-3' (forward) and 5'-AGGAGACCCCGGTTATGGAG-3' (reverse). These segments were electrophoresed by 5% PAGE. (D) Western blot analyses. Twenty micrograms of total cellular proteins from whole fish were electrophoresed through a denaturing polyacrylamide gel, electroblotted and hybridized with rabbit YARS2 antibody (1:1000 dilution) and GAPDH (1:8000 dilution) as a loading control.

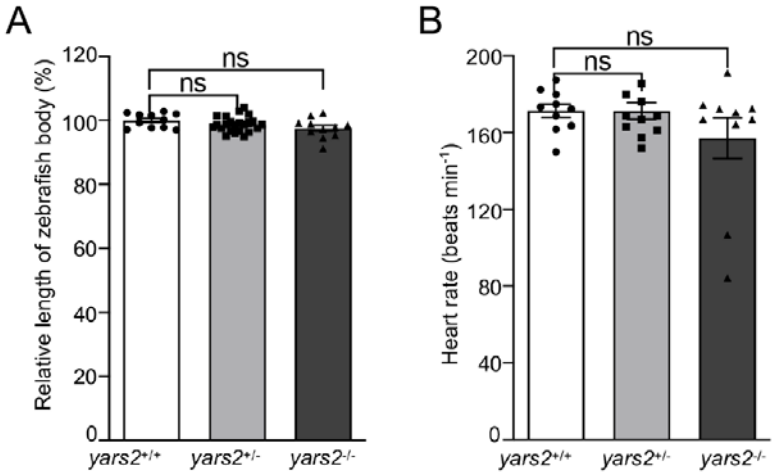

Figure S5 (related to Fig. 7). The *yars2* deletion did not significantly affect body length and heart rate in 5 dpf zebrafish. (A) Quantification of the body length of yars2$^{+/+}$ (n=11), yars2$^{+/-}$ (n=23) and yars2$^{-/-}$ (n=11) zebrafish. The values for the mutants were expressed as percentages of the average values for the wild type. (B) Heart beat frequency measured from yars2$^{+/+}$ (n=10), yars2$^{+/-}$ (n=11) and yars2$^{-/-}$ (n=10) zebrafish. Heart rates were measured by counting heartbeats during a 32-s interval at 5 dpf larva. The heart beats were counted by eye using a dissecting microscope (SMZ-1500, Nikon, USA). The error bars indicate standard deviations (SD) of the means. *, P<0.05; **, P<0.001; ***, P<0.0001; ns, no significant.

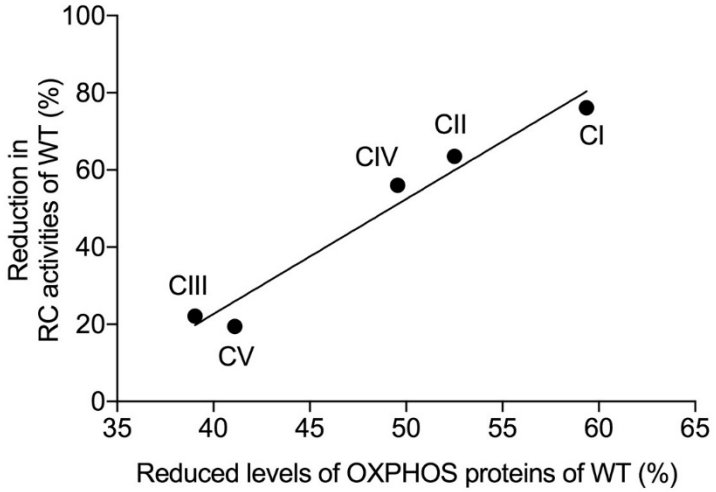

Figure S6. Correlation between the lower concentrations of OXPHOS proteins in the *YARS2*^{KO} cells and activities of the respiratory chain (RC) complexes. The average reduced levels of OXPHOS proteins [average levels of complex I (CI) (NDUF61, NDFUA9, NDUFS3 and NDUF8), complex II (CII) (SDHB), complex III (CIII)(CYTB, UQCRC1 and UQCRC2), complex IV (CIV) (CO2, COX5A and COX16) and complex V (CV) (ATP8)] and reduced activities of complex I, II, II, IV and V in *YARS2*^{KO} cells, expressed relative to the average value in the WT cells. Correlation analysis was performed using the Graphpad prism 8 program (Graphpad software). Statistical analysis was performed using the unpaired, two-tailed Student's t-test contained in contained in the Graphpad prism 8 program (Graphpad software).